

Hernquist model and central black holes detection through stellar kinematics

Roberto Infurna

1 Introduction

Stellar kinematics proves to be a diagnostic tool for the detection of black holes in the center of galaxies. In this work, I initialized Hernquist two-power model spherical galaxy (Binney & Tremaine, 2008):

$$\rho(r) = \frac{M}{2\pi a^3} \frac{1}{r \left(1 + \frac{r}{a}\right)^3} \quad (1)$$

Jeans theory prescribes the appropriate velocity distribution for the system to be in equilibrium. The Hernquist model is particularly useful because it accurately describes the surface brightness profile of many elliptical galaxies and has an easy analytic solution to the Eddington equation.

There is substantial evidence that most giant elliptical galaxies host supermassive black holes in their cores, and stellar kinematics has frequently been essential for their detection.

I sampled a Hernquist model galaxy at equilibrium, both with and without a central massive black hole. This task is more complex when a black hole is present, as the Eddington equation no longer has an analytic solution, requiring the distribution function to be computed numerically.

Finally, I used Jeans equations to assess under which observational conditions—particularly in terms of spatial and spectral resolution—the black hole can be significantly detected by means of stellar kinematics only.

2 Equilibria

For most practical uses stellar systems are approximated collisionless: star's orbits can be described as if the potential is generated by the smooth mass density distribution rather than each point-like source individually. The collisionless approximation holds as long as the system evolves for a time shorter than the relaxation time:

$$t_{relax} = \frac{0.1N}{\ln N} t_{cross} \quad (2)$$

where t_{cross} is the typical dynamical timescale of the galaxy (the time it takes a typical star to complete one orbit around the system). In any collisionless system it is useful to define the distribution function (DF). It expresses at any time t the probability of finding a randomly chosen star at point $\mathbf{w} = (\mathbf{x}, \mathbf{v})$ in phase space:

$$\int d^3x d^3v f(\mathbf{x}, \mathbf{v}, t) = 1 \quad (3)$$

The DF satisfies the collisionless Boltzmann equation, which represents the conservation of probability in phase space, analogous to how the continuity equation represents mass conservation:

$$\frac{\partial f}{\partial t} + \frac{\partial}{\partial \mathbf{w}} \cdot (f \dot{\mathbf{w}}) = 0 \quad (4)$$

Jeans theorem states that a solution of the collisionless Boltzmann equation is steady if and only if it depends on the phase space coordinates only through integrals of motion in the given potential. In any steady state potential $\Phi(\mathbf{x})$ the energy $H = \frac{1}{2}v^2 + \Phi(\mathbf{x})$ is an integral of motion. All stellar systems which DF is a function of the energy only are at equilibrium and are called ergodic. It's easy to prove that the mean velocity vanishes everywhere and the velocity dispersion is isotropic:

$$\sigma_{ij}^2 = \overline{v_i v_j} - \overline{v_i} \overline{v_j} = \overline{v_i v_j} = \sigma^2 \delta_{ij} \quad (5)$$

A self-consistent system is a system which density distribution generates the potential through Poisson's equation and the potential determines the density according to the collisionless Boltzmann equation. Hernquist mass distribution has spherical symmetry so it's most conveniently described by spherical coordinates. It's useful to define new variables:

$$\Psi = -\Phi + \Phi_0 \quad \mathcal{E} = -E + \Phi_0 = \Psi - \frac{1}{2}v^2 \quad (6)$$

Φ_0 is chosen such that $f > 0$ if $\mathcal{E} > 0$ and $f = 0$ if $\mathcal{E} \leq 0$. For an isolated system, $\Phi_0 = 0$ and the relative energy is equal to the binding energy. With this new coordinates Poisson's equation simply reads:

$$\nabla^2 \Psi = -4\pi G\rho \quad (7)$$

If the system is ergodic mass density satisfies:

$$\nu(r) = \frac{\rho(r)}{M} = \int_0^{\sqrt{2\Psi}} dv 4\pi v^2 f(\Psi - \frac{1}{2}v^2) = 4\pi \int_0^{\sqrt{2\Psi}} d\mathcal{E} f(\mathcal{E}) \sqrt{2(\Psi - \mathcal{E})} \quad (8)$$

Expressing ρ as a function of Ψ (Ψ is a monotonic function of ν):

$$\frac{1}{\sqrt{8\pi}} \nu(r) = 2 \int_0^{\Psi} d\mathcal{E} f(\mathcal{E}) \quad (9)$$

differentiating left and right and recognizing the resulting Abel integral equation, we finally get the Eddington formula, that permits to find a consistent DF for the given spherical distribution and potential:

$$f(\mathcal{E}) = \frac{1}{\sqrt{8\pi^2}} \int_0^{\mathcal{E}} \frac{d\Psi}{\sqrt{\mathcal{E} - \Psi}} \frac{d\nu}{d\Psi} \quad (10)$$

The only constrain is that the solution $f(\mathcal{E})$ must be nowhere negative and this happens only if the integral over energies in the Eddington formula is an increasing function of \mathcal{E} .

2.1 Hernquist at equilibrium

For a galaxy with density profile (1) the self consistent potential generated by Poisson's equation (7) is:

$$\Psi(r) = \frac{GM}{a} \frac{1}{(1 + \frac{r}{a})} \quad (11)$$

This is one of the few case in which Eddington's formula (10) has an analytic solution (Binney & Tremaine, 2008):

$$f(\mathcal{E}) = \frac{1}{\sqrt{2}(2\pi)^3(GMa)^{3/2}} \frac{\sqrt{\tilde{\mathcal{E}}}}{(1 - \tilde{\mathcal{E}})^2} \times \left[(1 - 2\tilde{\mathcal{E}})(8\tilde{\mathcal{E}}^2 - 8\tilde{\mathcal{E}} - 3) + \frac{3\sin^{-1}\sqrt{\tilde{\mathcal{E}}}}{\sqrt{\tilde{\mathcal{E}}(1 - \tilde{\mathcal{E}})}} \right] \quad (12)$$

where $\tilde{\mathcal{E}} = \mathcal{E}a/GM$.

To sample the mass distribution I first generated $N = M/(1M_{\odot})$ points with density profile (1) using the inverse Monte Carlo method. The task is straightforward because the mass integral is elementary and easily invertible:

$$\frac{M(r)}{M} = \int_0^{\infty} dr 4\pi r^2 \nu(r) = \frac{(r/a)^2}{(1 + r/a)^2} \quad (13)$$

To sample the velocity distribution I proceeded as follows: for each star I evaluated the potential $\Psi(r_*)$ and computed numerically the integral (8) for 1000 values of \mathcal{E} in the range $(0, \Psi(r_*))$, with DF given by (12). Then I performed inverse Monte Carlo again: I extracted a number from a uniform PDF between 0 and $\nu(r_*)$ and find through an interpolation the corresponding value of the integral (8), which in turns gives the star's energy and finally the magnitude of velocity. The directions of the velocity vectors are sampled from a unit sphere, as for the position vectors.

To further verify whether the positions and velocities are consistent with the Hernquist model and equilibrium, I compared the sampled distributions with the theoretical ones. The star radii and energies were binned into 10 intervals to generate two histograms. To recover the mass density and distribution function, it is necessary to normalize each bin's count by the volume of that bin. For the mass distribution, this are the volumes of the spherical shells: $\frac{4\pi}{3}(R_{i+1}^3 - R_i^3)$. The volume of an energy bin in phase space is a bit more subtle:

$$\Omega(\mathcal{E}_i, \mathcal{E}_{i+1}) = \int \int 4\pi r^2 dr 4\pi v^2 dv \Theta(\mathcal{E}_i - \Psi(r) + v^2/2) \Theta(\Psi(r) - v^2/2 - \mathcal{E}_{i+1}) \quad (14)$$

this integral can be also written:

$$16\pi^2 \int \int r^2 dr \sqrt{2(\Psi(r) - \mathcal{E})} d\mathcal{E} = 16\pi^2 \int_{\mathcal{E}_i}^{\mathcal{E}_{i+1}} d\mathcal{E} \int_0^{\infty} r^2 dr \sqrt{2(\Psi(r) - \mathcal{E})} \quad (15)$$

The consistency between the energy sampling and the distribution function is sufficient to verify that the system is in equilibrium.

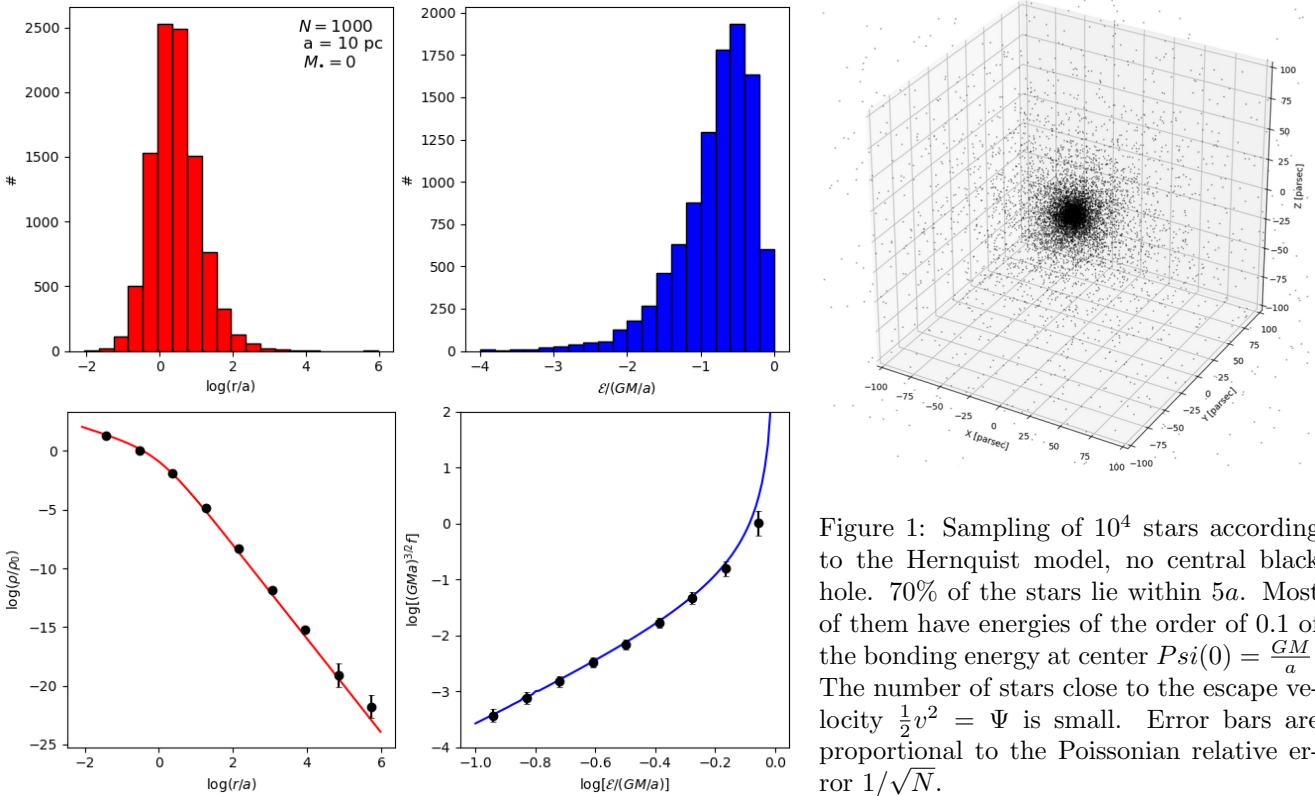


Figure 1: Sampling of 10^4 stars according to the Hernquist model, no central black hole. 70% of the stars lie within $5a$. Most of them have energies of the order of 0.1 of the bonding energy at center $\Psi(0) = \frac{GM}{a}$. The number of stars close to the escape velocity $\frac{1}{2}v^2 = \Psi$ is small. Error bars are proportional to the Poissonian relative error $1/\sqrt{N}$.

2.2 Equilibrium with central black hole

The central black hole makes the problem more complicated: the density distribution doesn't change, but the potential does:

$$\Phi(r) = \Phi_{gal}(r) + \Phi_{BH}(r) = -\frac{GM_{gal}}{a} \frac{1}{(1 + \frac{r}{a})} - \frac{GM_\bullet}{r} \quad (16)$$

as a consequence the DF given by (12) doesn't solve Eddington formula (10) any more and if the star's velocities were initialized as before the system would be out of equilibrium. A new DF must be computed for the composite potential. This time an analytic solution to Eddington's formula does not exist and the only way is to proceed numerically. I generated a sufficiently dense grid of radii (in logarithmic scale) and computed density and potential. I took the differences and compute the ratios. The derivative $d\nu/d\Psi$ is obtained interpolating on this array. I generated an array of energies and for each computed numerically the integral:

$$\int_0^\mathcal{E} \frac{d\Psi}{\sqrt{\mathcal{E} - \Psi}} \frac{d\nu}{d\Psi} \quad (17)$$

Finally I took the differences between the integrals and divide by the energy increment. The DF is obtained interpolating on this array. Once the new DF is known the distribution sampling can proceed exactly as described in the previous section.

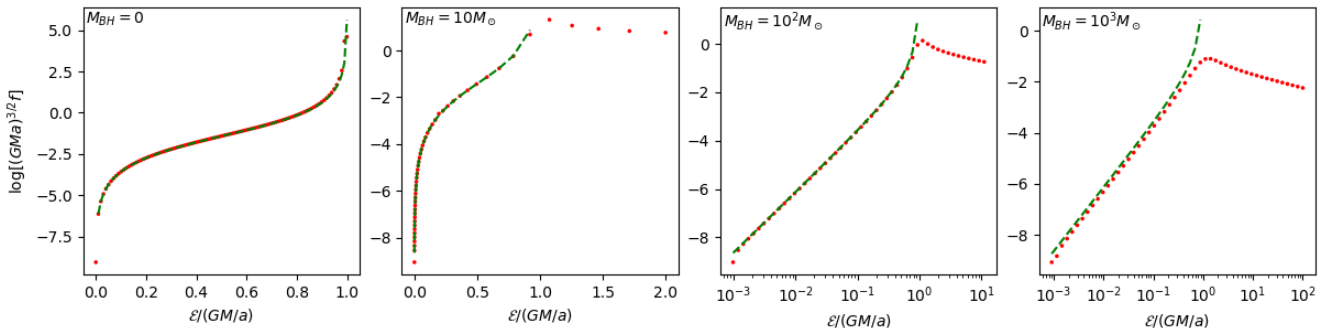


Figure 2: Numerical DF obtained from Eddington's formula (10) for systems of 10^4 stars and central black hole of $0, 10^{-3}, 10^{-2}$ and 10^{-1} the galactic mass. The analytic DF for the model with no black hole is plotted in green.

Hernquist model allows a solution at equilibrium with a central black hole since the integral (17) is an increasing function of \mathcal{E} . This is not always true, for example Plummer model can not host a central black hole and be at equilibrium at the same time.

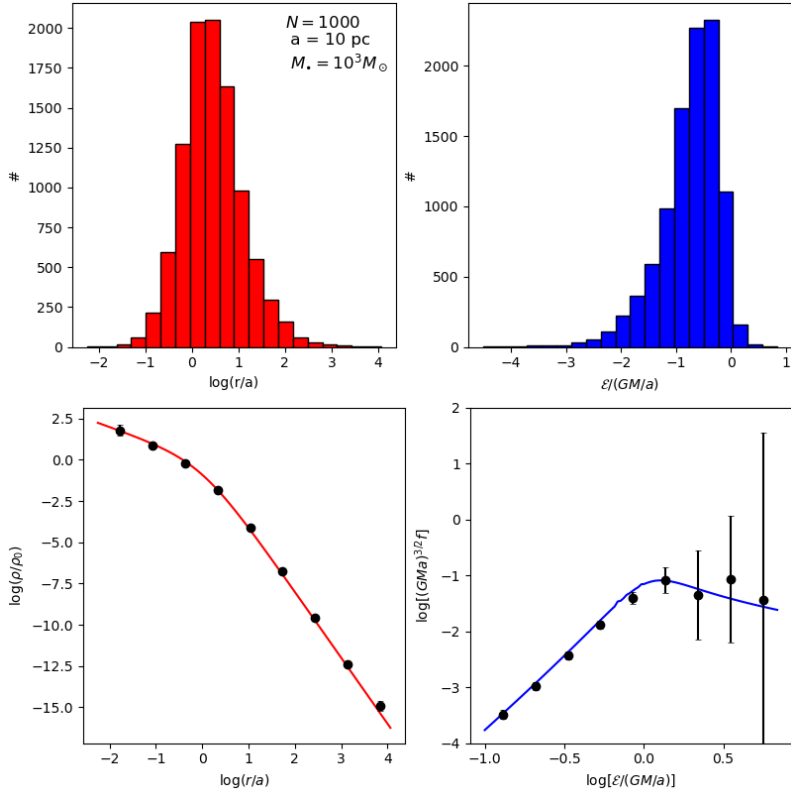


Figure 3: Sampling from Hernquist model of 10^4 stars, with central black hole of 10^{-1} times the galactic mass. Due to the deep gravitational well of the black hole, the closest stars will find themselves in highly bound orbits ($\mathcal{E} > \frac{GM}{a}$).

3 Evolution

I initialized a hernquist galaxy of 10000 stars with scale radius $a = 10$ pc and central black hole of $10^3 M_\odot = 10^{-1} M_{gal}$. To assess whether equilibrium is achieved, I evolved the system using Barnes’s treecode software (<https://legacy.ifa.hawaii.edu/faculty/barnes/treecode/treeguide.html>). Some attention must be paid to the parameter settings. Treecode provides reliable results only if the time increment is very small compared to the dynamical timescale. A good estimate of dynamical time is the time it takes for a typical star to complete a circular orbit: $t_{dyn} \sim \frac{2\pi r}{v_{circ}}$, where v_{circ} is the circular velocity and for a spherically symmetric potential is:

$$v_{circ} = \sqrt{r \frac{d\Phi}{dr}} = \sqrt{\frac{GM(r)}{r}} \quad (18)$$

For our galaxy shortest and longest orbital times are 0.002 and 2×10^6 internal units ($G = 1$, mass expressed in units of solar mass and lengths expressed in units of parsec), or 10^{-2} and 2×10^5 Myrs. The median is 12 (0.82 Myrs), and it is a good estimate of the galactic dynamical timescale. A suitable time step for evolving the system is 0.0002, which is 10^{-5} times the typical orbital period and 1/10 of the shortest orbital period.

One issue with algorithms that use non-adaptive time steps, such as treecode, is that the force between two particles diverges when the distance between them becomes very small. While this is physical, it can have deleterious effects on numerical integration. To address this, a softening parameter ϵ is introduced in the gravitational force. I set ϵ 1/10 of the smallest separation between a star and the central black hole, which is 0.2.

A prediction that can be verified with treecode is whether the stars falling within the black hole’s dynamical radius have nearly Keplerian orbits. The black hole’s dynamical radius is defined as the radius where the enclosed galactic mass equals the mass of the black hole (Binney & Tremaine, 2008):

$$M(r) = M_{gal} \frac{(r/a)^2}{(1+r/a)^2} = M_\bullet \quad (19)$$

This radius marks the region of the galaxy where the dynamics is dominated by the black hole. For a galaxy of $M = 10^4 M_\odot$, $a = 10$ pc and $M_\bullet = 10^3 M_\odot$ the dynamical radius is at $0.3a$. If the black hole mass is $10^2 M_\odot$ it is at $0.1a$.

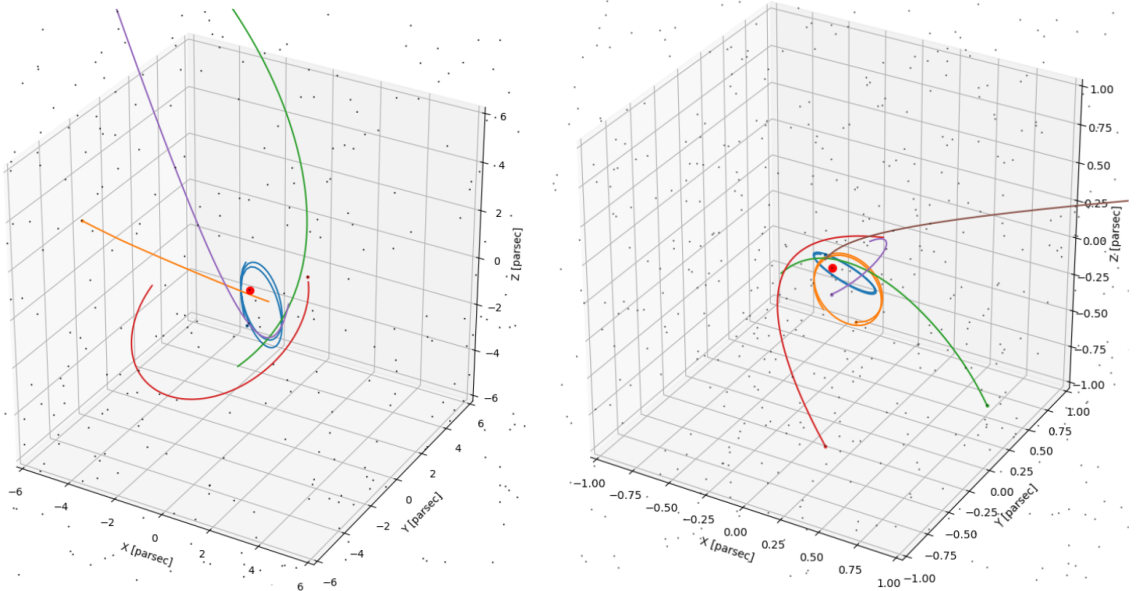


Figure 4: Keplerian orbits of some stars inside the dynamical radius of a black hole of $10^3 M_\odot$.

4 Black hole detection through stellar kinematics

Few observables provide significant insights into the dynamics of a galaxy. The most crucial among these are surface brightness, line-of-sight (LOS) velocity, and line-of-sight velocity dispersion. Surface brightness, under the assumption of a uniform mass-to-light ratio, is indicative of the mass distribution. The LOS velocity reveals the rotation of the galaxy, while the LOS velocity dispersion offers information about the random motions of stars within the galaxy. Surface brightness is measured through photometry, whereas the mean velocity and velocity dispersion are obtained via spatially resolved spectroscopic measurements of the shift and width of stellar lines, respectively.

For spherically symmetric galaxies, surface brightness is given by:

$$I(R) = \frac{1}{\Upsilon} \int_{-\infty}^{+\infty} dx_{\parallel} \rho(r) = \frac{2}{\Upsilon} \int_R^{\infty} \rho(r) \frac{r dr}{\sqrt{r^2 - R^2}} \quad (20)$$

where Υ is the mass-to-light ratio and R is the projected distance from the center of the spheroid in the plane of the sky. Similarly, the line of sight velocity dispersion for an isotropic spherical system is:

$$\sigma_{\parallel}^2(R) = \frac{2}{\Upsilon I(R)} \int_R^{\infty} \sigma^2(r) \rho(r) \frac{r dr}{\sqrt{r^2 - R^2}} \quad (21)$$

where $\sigma^2 = \overline{v_r^2}$ for an isotropic system. The moments of the distribution such as \bar{v} and $\overline{v_r^2}$ can be recovered directly from the DF or by solving Jeans equations. This second way is often more convenient because it does not require the knowledge of the DF. For a spherical ergodic system $\bar{v} = 0$ everywhere and the equation for $\overline{v_r^2}$ is particularly simple:

$$\frac{d(\rho \overline{v_r^2})}{dr} = -\rho \frac{d\Phi}{dr} \quad (22)$$

with the boundary condition at infinity $\rho \overline{v_r^2} = 0$. It resembles the hydrostatic equilibrium equation for a collisional gas, with $\rho \overline{v_r^2}$ acting like the pressure term (Tremaine *et al.*, 1994).

Expanding equation (22):

$$\frac{d}{dr} v_r^2 + \frac{d \ln \rho}{dr} v_r^2 = -\frac{d\Phi}{dr} \quad (23)$$

which is a Cauchy differential linear first order equation with solution (Binney & Tremaine, 2008):

$$\overline{v_r^2}(r) = \frac{GM_{gal}}{a} \left[(1+6\mu)xy^3 \ln(y/x) - \mu y^3(3x - \frac{1}{2})/x - x[\frac{1}{4} + \frac{1}{3}y + \frac{1+\mu}{2}y^2 + (1+3\mu)y^3]/x \right] \quad (24)$$

where $x = r/a$, $y = 1+x$, $\mu = M_\bullet/M_{gal}$. It's worth noticing that having already computed the DF we could have also employed the definition of the moments of the distribution.

I considered two Hernquist galaxies initialized at equilibrium, each of mass $10^4 M_\odot$ and $a = 10$ pc, and with central black holes of $10^2 M_\odot$ and $10^3 M_\odot$ respectively. I then used the solution for σ_{\parallel} (equations (21) and (24)) to

determine the conditions under which the black hole is detectable via stellar kinematics, focusing on the precision with which the black hole's mass can be inferred.

First, I defined a range of projected distance from center bins with a resolution Δr . The resolution will prove to be crucial for the significance of black hole detection and mass estimation. For each radial bin, I selected the stars within it and computed their LOS velocities by projecting the velocity onto the vector $(0, 0, -1)$ (line of sight parallel to z-axis). The standard deviation of these velocities provided the LOS velocity dispersion.

In the case of a $10^3 M_\odot = 0.1 \times M_{gal}$ central black hole, Fig. 5 show that low-resolution measurements are sufficient to confirm the presence of a massive black hole. However, estimating its mass accurately requires resolving at least the dynamical radius. For a less massive black hole of $10^2 M_\odot = 0.01 \times M_{gal}$, Fig. 6 the situation is different. Low-resolution measurements cannot see the black hole at all, making high-resolution measurements necessary not only for precise mass estimation but also for detection.

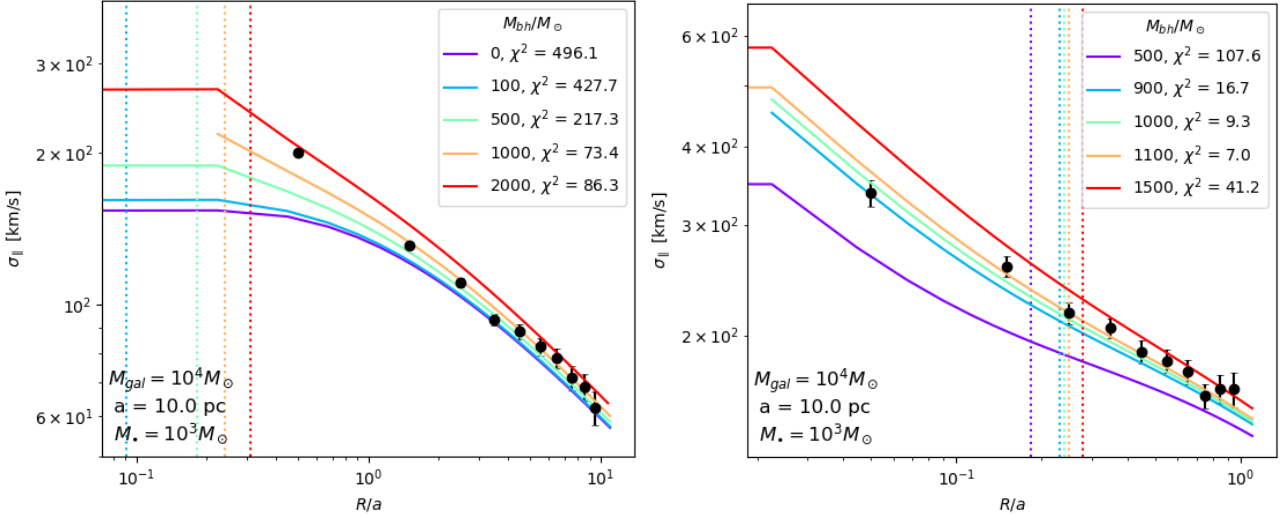


Figure 5: Comparison between the analytic curves of LOS velocity dispersion versus R for different values of the central black hole's mass and the data points from the simulated Hernquist galaxy with a central black hole of $10^3 M_\odot$. The galaxy's mass is $10^4 M_\odot$ with a scale radius of $a = 10$ pc. The left panel displays a low-resolution measurement with radial bins of width a extended up to $10a$. The right panel shows a high-resolution measurement of the innermost part of the galaxy, with radial bins of width $0.1a$. Dotted lines indicate the dynamical radii of the black holes. Error bars represent the uncertainties in the standard deviations and are calculated using the formula: $\sigma_{\sigma_{\parallel}} = \frac{\sigma_{\parallel}}{\sqrt{2(N-1)}}$.

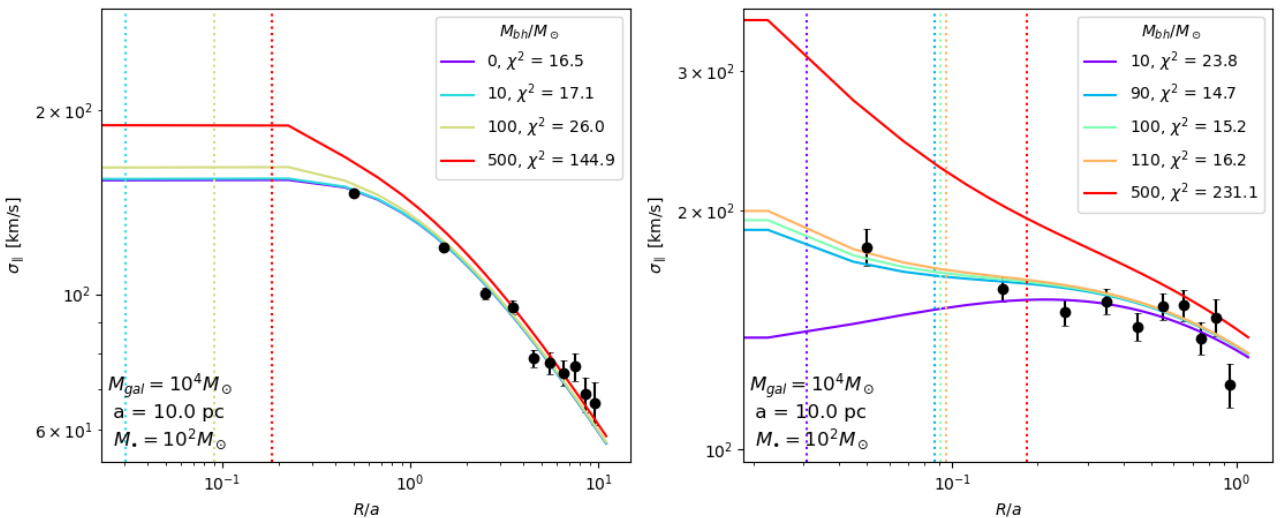


Figure 6: The same Hernquist galaxy but with central black hole of $10^2 M_\odot = 0.01 \times M_{galaxy}$.

5 Projection in sky

I simulated how the galaxy would appear to a telescope with given sensitivity, angular resolution, and spectral resolution, and under what conditions the black hole is detectable. To project the galaxy in the sky, I took the scalar product of the position vector with $(0, 1, 0)$ and $(1, 0, 0)$ to obtain the right ascension (RA) and declination (DEC), and with $(0, 0, 1)$ for the line-of-sight component (aligned with the z-axis). I initialized a Hernquist galaxy of mass $10^4 M_\odot$ and of scale length $a = 10$ pc, and with a central black hole of $10^3 M_\odot$. The galaxy is located 1 Mpc from Earth. At this distance, the innermost region of 10 pc radius has an angular size of $\sim 4''$. I set the telescope's angular resolution $1''$. The field of view (FOV) is $100''$ and covers ~ 250 pc $\sim 25a$ including $\sim 90\%$ of the mass of the galaxy. The spectral resolution is crucial. It is defined as:

$$R = \frac{\lambda}{\Delta\lambda} = \frac{c}{\Delta v} \quad (25)$$

To measure the random motion of stars with an accuracy of approximately 10 km/s, a spectral resolution of at least 30,000 is required. This level of resolution is typical for high-resolution spectrometers such as HARPS and UVES. In contrast, SDSS spectrographs, which have a spectral resolution of about 2,000, cannot resolve velocities smaller than 150 km/s. Therefore, for detecting black holes through stellar kinematics, high-resolution spectrometers are essential.

As previously discussed, for a central black hole with a mass of $10^3 M_\odot$, low spatial resolution does not provide accurate mass measurements. To address this, I simulated a second observation focusing on the inner part of the galaxy ($r < 8$ pc), with angular resolution of $0.1''$ (comparable to HST) and a FOV of $3''$.

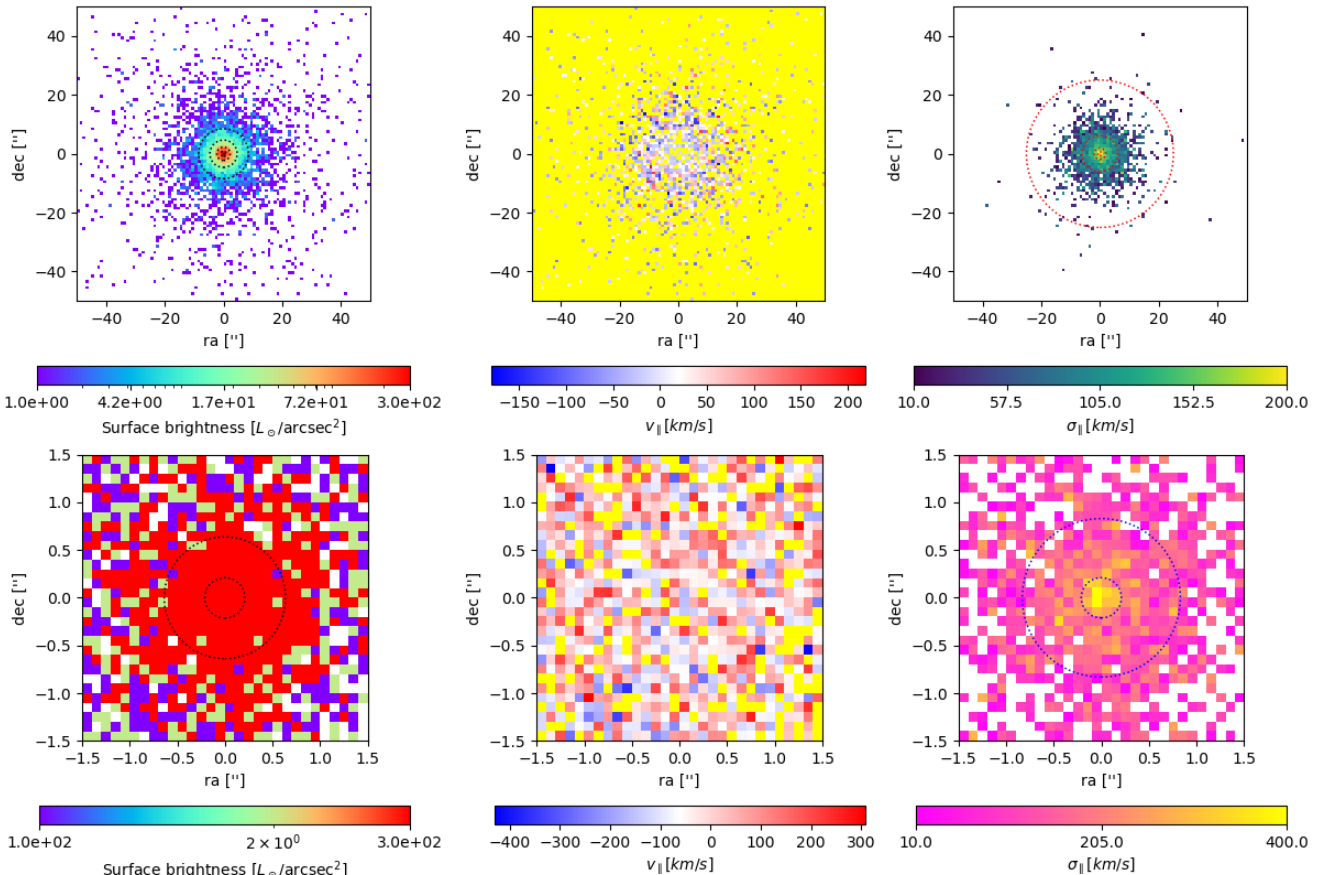


Figure 7: Two simulations of how a Hernquist galaxy with a mass of $M = 10^4 M_\odot$, a scale length of 10 pc, and a central black hole $M_\bullet = 10^3 M_\odot$, located 1 Mpc from Earth, would appear when observed with two telescopes, both having a high spectral resolution of 30,000. The first telescope has angular resolution $1''$ and FOV $100''$, while the second telescope has angular resolution $0.1''$ and FOV $3''$. The circles represent lines of constant theoretical surface brightness and LOS dispersion. With a spectral resolution below 1,000, central and right panels would not reveal any discernible features.

I computed the χ^2 value by comparing the observed line-of-sight (LOS) velocity dispersion with the predicted dispersion (as given in equation (21)), but only for bins containing more than 10 stars. I adjusted the error by

adding the spectral resolution in quadrature:

$$\sigma_{\sigma_{\parallel}} = \sqrt{\left(\frac{\sigma_{\parallel}}{\sqrt{2(1-N)}}\right)^2 + \Delta_v^2} \quad (26)$$

The high spatial resolution test allows for a significant determination of the central black hole's mass ($M_{\bullet} = 10^3 M_{\odot}$ gives $\chi^2 = 31$ with 27 d.o.f., whereas $M_{\bullet} = 10^3 M_{\odot}$ and $M_{\bullet} = 10^3 M_{\odot}$ give $\chi^2 > 70$).

References

- [1] J. Binney & S. Tremaine *Galactic Dynamics*(2008)
- [2] Tremaine et al. *A family of models for spherical stellar systems* (1994)